



Ghrelin protects against lipopolysaccharide-induced acute respiratory distress syndrome through the PI3K/AKT pathway

Received for publication, April 17, 2021, and in revised form, August 11, 2021. Published, Papers in Press, August 23, 2021.
<https://doi.org/10.1016/j.jbc.2021.101111>

Lishan Zhang^{1,2,‡}, Shanhui Ge^{1,2,‡}, Wanmei He^{1,2}, Qingui Chen^{1,2}, Caixia Xu^{3,*}, and Mian Zeng^{1,2,*}

From the ¹Department of Medical Intensive Care Unit, The First Affiliated Hospital, ²Institute of Pulmonary Diseases, ³Research Center of Translational Medicine, The First Affiliated Hospital, Sun Yat-Sen University, Guangzhou, China

Edited by Dennis Voelker

Pulmonary endothelial barrier dysfunction is a major pathophysiology observed in acute respiratory distress syndrome (ARDS). Ghrelin, a key regulator of metabolism, has been shown to play protective roles in the respiratory system. However, its effects on lipopolysaccharide (LPS)-induced pulmonary endothelial barrier injury are unknown. In this study, the effects of ghrelin on LPS-induced ARDS and endothelial cell injury were evaluated *in vivo* and *in vitro*. *In vivo*, mice treated with LPS (3 mg/kg intranasal application) were used to establish the ARDS model. Annexin V/propidium iodide apoptosis assay, scratch-wound assay, tube formation assay, transwell permeability assay, and Western blotting experiment were performed to reveal *in vitro* effects and underlying mechanisms of ghrelin on endothelial barrier function. Our results showed that ghrelin had protective effects on LPS-induced ARDS and endothelial barrier disruption by inhibiting apoptosis, promoting cell migration and tube formation, and activating the PI3K/AKT signaling pathway. Furthermore, ghrelin stabilized LPS-induced endothelial barrier function by decreasing endothelial permeability and increasing the expression of the intercellular junction protein vascular endothelial cadherin. LY294002, a specific inhibitor of the PI3K pathway, reversed the protective effects of ghrelin on the endothelial cell barrier. In conclusion, our findings indicated that ghrelin protected against LPS-induced ARDS by impairing the pulmonary endothelial barrier partly through activating the PI3K/AKT pathway. Thus, ghrelin may be a valuable therapeutic strategy for the prevention or treatment of ARDS.

Acute respiratory distress syndrome (ARDS) is a rapidly progressive disease that usually occurs in the intensive critical care unit; given the limited availability of effective treatments for ARDS, more progress is needed to further reduce mortality and morbidity from ARDS.

Disorders of pulmonary endothelial barrier function are pivotal early steps in the occurrence and development of ARDS. Disruption of the endothelial cell barrier leads to vascular hyperpermeability and leakage of albumin and fluid, resulting in tissue edema, which is a characteristic of ARDS

(1–3). Both cell–cell junction disruption and decreased endothelial cell numbers contribute to pulmonary endothelial barrier disruption (4). Previous studies have shown that lipopolysaccharide (LPS) has dual effects on pulmonary endothelial cell barrier function through the PI3K/AKT signaling pathway. High doses of LPS inhibit human pulmonary microvascular endothelial cell migration, reduce the expression of vascular endothelial cadherin (VE-cadherin) protein, and block AKT phosphorylation, whereas low doses have the opposite effects (5). Similarly, several studies have suggested that changes in cell migration, intercellular junction formation, and cell differentiation, which are associated with endothelial barrier, are mediated by the PI3K/AKT pathway (6, 7).

Ghrelin, a gastrointestinal hormone peptide, has attracted much attention because of its ability to affect different types of systems (2). Notably, several studies have shown that ghrelin plays protective roles in animal lung injury models (8–10). Our previous studies also showed that ghrelin suppresses apoptosis in alveolar macrophages by inhibiting the c-Jun N-terminal kinase and Wnt/ β -catenin signaling pathways (11). As an endogenous growth factor, ghrelin promotes cell migration and cell proliferation *via* the PI3K/AKT pathway in intestinal epithelial cells, A549 human lung cancer cells, and renal cells (12–14). However, it is unclear whether ghrelin has positive effects on impairment of lung endothelial cell injury through the PI3K/AKT pathway.

Accordingly, in this study, we investigated the roles and mechanism of ghrelin in lung endothelial cell injury in LPS-induced ARDS and explored the roles of the PI3K/AKT signaling pathway in mediating the effects of ghrelin. Our results provided important insights into the roles of ghrelin in protecting the endothelial cell barrier against LPS-induced barrier disruption through the PI3K/AKT pathway and suggested that ghrelin may be a potential therapeutic target in the treatment of ARDS.

Results

Ghrelin attenuated pathological changes and pulmonary endothelial cell injury in a mouse model of LPS-induced ARDS

We used a mouse model of LPS-induced ARDS to examine whether ghrelin administration could affect the progression of LPS-induced ARDS. As shown in [Figure 1](#), administration of LPS alone into the lungs of mice resulted

[‡] These authors contributed equally to this work.

* For correspondence: Mian Zeng, zengmian@mail.sysu.edu.cn; Caixia Xu, xucx3@mail.sysu.edu.cn.

Ghrelin, acute respiratory distress syndrome

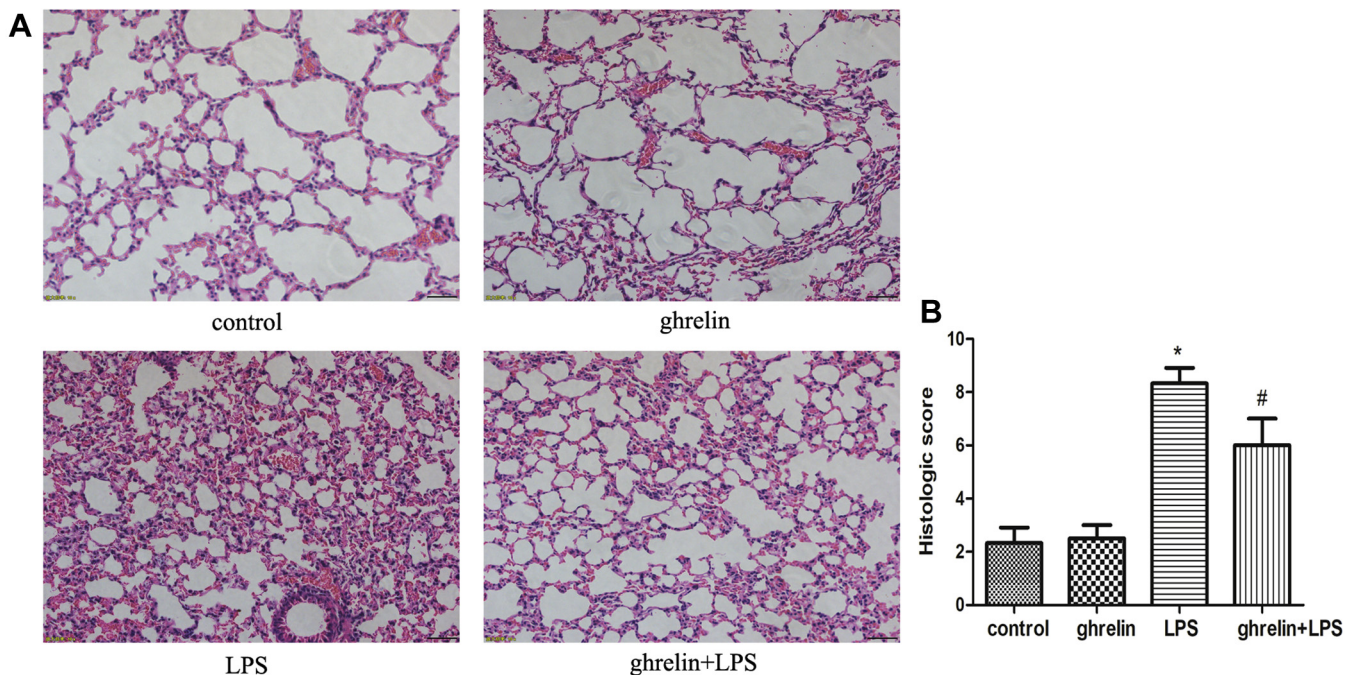


Figure 1. Ghrelin attenuates LPS-induced lung pathological alterations. Histopathological changes of lungs determined by H&E staining ($\times 200$). Male Balb/c mice were randomized into control, ghrelin, LPS, and ghrelin + LPS groups ($n = 6$, each group analyzed in triplicate). Lung histological changes were assessed 24 h after LPS instillation as described in [Experimental procedures](#). *A*, representative images of H&E-stained sections of lung tissues for control, ghrelin, LPS, and ghrelin + LPS group. *B*, pathological scores of lung samples in each group are shown, indicating that treatment with ghrelin significantly ameliorates LPS-induced lung edema, hemorrhage, alveolar collapse, and inflammatory cell infiltration. Three slices of each mouse were used, and the observer randomly observed and photographed six fields of view. The observers were blinded to each experimental group. ($n = 6$, $*p < 0.05$ compared with the control group, $\#p < 0.05$ compared with the LPS group). LPS, lipopolysaccharide.

in pathological changes, including significant inflammatory cell infiltration, interstitial and intra-alveolar edema, hemorrhage, interalveolar septal thickening, alveolar collapse, and destruction of lung structure, compared with that in mice receiving saline or ghrelin only. Compared with the LPS group, the ghrelin-pretreated group exhibited marked improvement in lung architecture, reduced alveolar edema and hemorrhage, decreased inflammatory cell infiltration, and lower lung injury scores (Fig. 1A). Three parameters including hemorrhage, edema, and leukocyte infiltration were used as the criteria for lung injury, and the total score of these parameters was calculated according to the above system (0 points for nonexistent, 1 point for mild, 2 points

for moderate, and 3 points for severe). The results of lung damage scores implied that the efficacy of ghrelin was statistically significant (Fig. 1B).

Working concentrations of LPS and ghrelin

Cell viability was measured using Cell Counting Kit-8 (CCK-8) assays to identify the concentrations of LPS and ghrelin for subsequent experiments. LPS decreased cell viability in a concentration- and time-dependent manner, with a half-maximal inhibitory concentration of 150 $\mu\text{g/ml}$, for 24 h (Fig. 2A). Ghrelin increases cell viability in a concentration-dependent manner, with a significant increase observed at

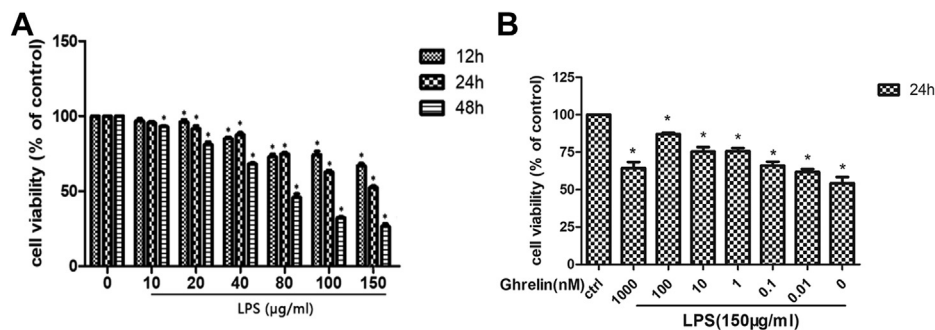


Figure 2. Effect of LPS and ghrelin on cell viability. *A* and *B*, viability of EA.hy 926 cells was estimated using the Cell Counting Kit-8 assay. Cells were cultured in DMEM with different concentration of LPS, with a median inhibitory concentration (IC_{50}) value of 150 $\mu\text{g/ml}$ for 24 h. Later, cells were stimulated with 150 $\mu\text{g/ml}$ LPS alone or in the presence of the indicated concentrations of ghrelin. According to the result, ghrelin at 100 nM plays a significant role on cell viability. Representative of three independent experiments, mean \pm SEM, $*p < 0.05$ versus control. DMEM, Dulbecco's modified Eagle's medium; LPS, lipopolysaccharide.

100 nM (Fig. 2B). From these results, we selected 150 µg/ml LPS and 100 nM ghrelin as working concentrations for subsequent experiments.

Effect of ghrelin on LPS-induced apoptosis in endothelial cells

Next, we evaluated the effects of ghrelin on LPS-induced apoptosis. We randomly observed and photographed four fields of view and counted the number of each view. The number of cells in each field ranges from 150 to 200. Because LPS can cause cell shrinkage and apoptosis, the cells in the LPS group are smaller than other groups, and more cells are observed in the same field of view. However, this did not affect the results because the percentage of apoptosis in each field of view was observed. The results of TUNEL staining showed that there were fewer apoptotic cells in both the control and ghrelin groups, whereas the number of apoptotic cells in the LPS group increased significantly (Fig. 3, A–C). Compared with the LPS group, pretreatment with 100 nM ghrelin caused an obvious decrease in the number of TUNEL-positive cells (Fig. 3D).

Annexin V-FITC and propidium iodide (PI) dual staining showed that the percentage of apoptotic cells was higher in the LPS group than in the untreated control group (3.7% versus 22.31%, respectively; $p < 0.05$). Moreover, an evidently lower percentage of apoptotic cells was observed after ghrelin pretreatment than that after LPS treatment alone (10.56% versus 22.31%, respectively; $p < 0.05$; Fig. 3, B and D). Furthermore, Western blotting showed that ghrelin reduced the expression of Bax protein and increased Bcl-2 expression compared with that in the LPS group, indicating that apoptosis was inhibited (Fig. 3, E and F). Both TUNEL staining and flow cytometry analysis demonstrated that ghrelin markedly suppressed endothelial cell apoptosis induced by LPS, as supported by the reduced expression of Bax protein and increased expression of Bcl-2 protein (Fig. 3, A–F).

Ghrelin improved endothelial cell barrier function impaired by LPS

In vitro scratch-wound healing tests were conducted to evaluate the effects of ghrelin on the migration of endothelial cells. The results showed that wounds in the ghrelin + LPS group recovered more significantly than those in the LPS group at 24 h after scratching (Fig. 4A).

Next, to evaluate the roles of ghrelin in angiogenesis *in vitro*, tube formation of endothelial cells was assessed. Compared with the control group, the LPS group showed almost no tubular structure formation. However, tube formation was observed when cells were pretreated with ghrelin before LPS treatment. Thus, these results indicated that ghrelin significantly increased tube formation and branching (Fig. 4B).

We then examined whether ghrelin decreased the permeability of EA.hy 926 cells using Transwell permeability assays (Fig. 5, A and B). Our findings showed that addition of ghrelin significantly blocked the LPS-induced disruption of cell

permeability compared with that in the LPS group. Importantly, high-permeability pulmonary edema is attributed to disruption of endothelial adhesion junctions, which contain the transmembrane adhesion protein VE-cadherin. In this study, our Western blotting results demonstrated that EA.hy 926 cells exposed to LPS exhibited reduced VE-cadherin protein expression, whereas administration of ghrelin reversed the harmful effects of LPS on EA.hy 926 cells, as supported by an increase in the total abundance of VE-cadherin protein (Fig. 5, C and D). Taken together, these findings showed that ghrelin reinforced the pulmonary endothelial cell barrier by promoting cell migration and tube formation and stabilizing adherens junctions.

PI3K/AKT signaling contributed to ghrelin-mediated protection of lung injury in vitro and in vivo

To evaluate the effects of ghrelin on AKT-related signal activation *in vitro*, phosphorylation of PI3K and AKT was assessed by Western blotting. We found that LPS decreased PI3K and AKT phosphorylation compared with that in the control group, whereas ghrelin pretreatment obviously increased PI3K and AKT phosphorylation. As expected, we observed that LY294002 inhibited the stimulation of PI3K and AKT phosphorylation by ghrelin (Fig. 6, A and B). These results indicated that ghrelin was a stimulatory factor for PI3K/AKT signaling pathways.

To clarify whether PI3K/AKT activation was involved in mediating the protective effects of ghrelin *in vitro*, EA.hy 926 cells were treated with LY294002 1 h before LPS challenge. We observed that changes in the levels of Bax and Bcl-2 proteins were reversed after treatment with LY294002, indicating that the antiapoptotic effects of ghrelin were markedly reduced by addition of the PI3K inhibitor LY294002 (Fig. 6, C and D). Moreover, LY294002 also reversed the stimulatory effects of ghrelin on cell migration and differentiation after LPS treatment (Fig. 6, E–H). Therefore, these findings suggested that ghrelin may play a protective role in endothelial cells, at least partially through PI3K/AKT signaling.

To confirm the relationship between ghrelin and PI3K/AKT signaling pathways *in vivo*, lung staining with “p-Akt antibody” was performed. We found that the expression of p-Akt was increased in the ghrelin group while decreased in the LPS group (Fig. 7, A and B). *In vivo*, before exposure to LPS, mice were pretreated with the PI3K inhibitor LY294002 to confirm that PI3K/AKT signaling was involved in ghrelin-mediated LPS-induced ARDS *in vivo*. Indeed, our findings demonstrated that pretreatment with LY294002 aggravated histological injury in ghrelin-pretreated mice after LPS challenge (Fig. 7, C and D). To further explore the effects of LPS on pulmonary endothelial cells and clarify whether ghrelin played a preventive effect in LPS-induced ARDS by affecting the endothelial cell barrier, VE-cadherin protein immunofluorescence was conducted because VE-cadherin functions to maintain vascular integrity. The immunofluorescence results

Ghrelin, acute respiratory distress syndrome

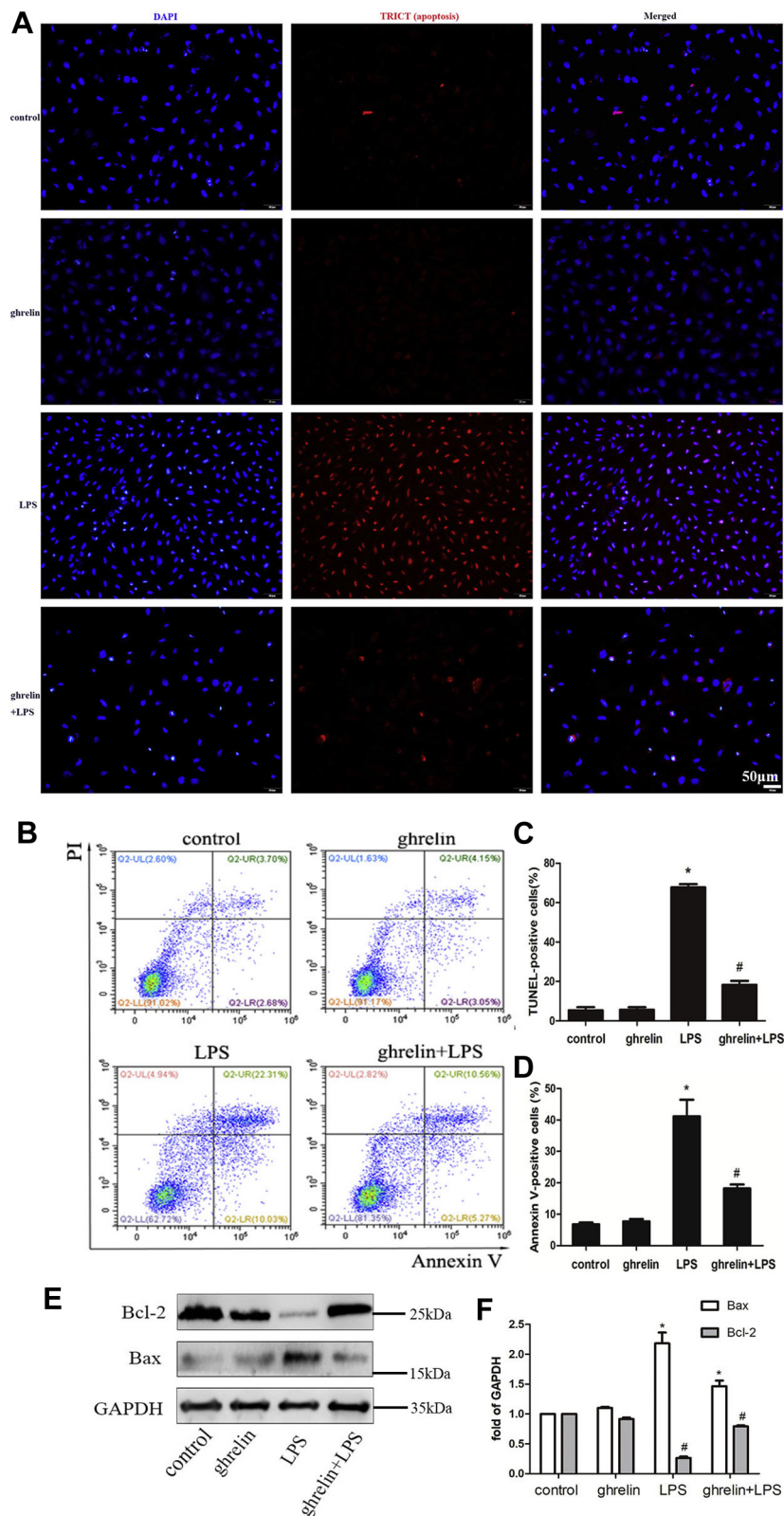


Figure 3. Ghrelin plays an antiapoptotic effect after LPS insults in EA.hy 926 cells. *A*, representative image of TUNEL assay in LPS-treated cells at 24 h. Apoptotic cells are quantified by counting the percentages of TUNEL-positive nuclei. *B*, detection of early and late apoptosis of cells after 24-h treatment with LPS was analyzed with Annexin V-FITC and PI staining through the flow cytometer. *C* and *D*, quantitative analysis of the ratios of apoptotic cells is shown in the bar graphs. Both the TUNEL assay and flow cytometer demonstrated that addition of ghrelin diminished the ratios of TUNEL-positive cells and apoptotic cells under LPS insult condition. *E*, Western blot analysis shown that ghrelin increased the level of antiapoptotic protein Bcl-2 under LPS exposure, as well as reduces the level of proapoptotic protein Bax. *F*, quantification of Bcl-2 and Bax expression by densitometric analysis. Data are presented as the mean \pm SEM, $n = 4$, * $p < 0.05$ compared with the control group, # $p < 0.05$ compared with the LPS group. LPS, lipopolysaccharide; PI, propidium iodide.

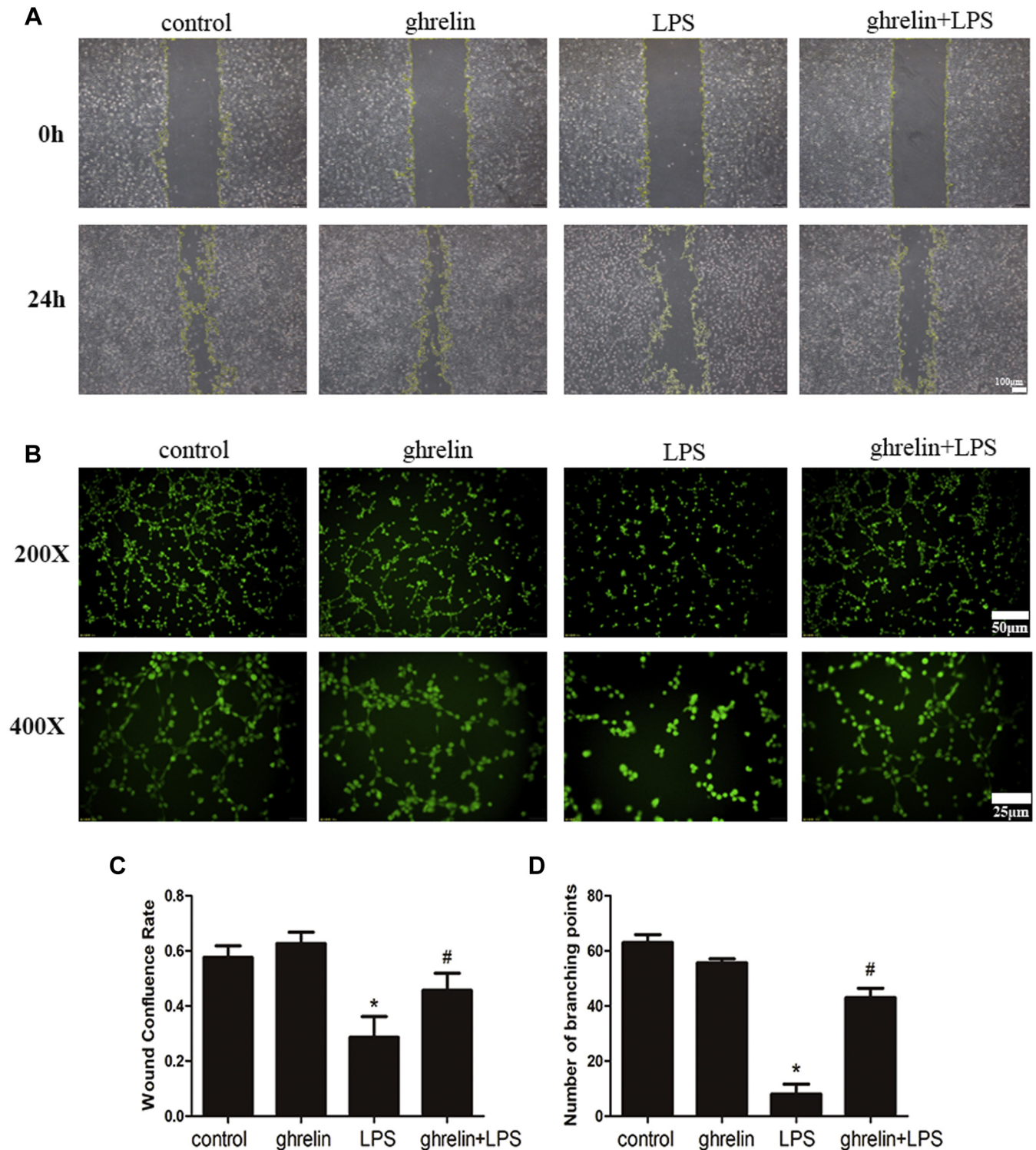


Figure 4. Ghrelin improved endothelial cell migration and differentiation ability impaired by LPS. *A*, effect of ghrelin at a concentration of 100 nM on the migration of endothelial cells. Cells were divided into four groups, the control group, ghrelin group, LPS group, and ghrelin + LPS group. Yellow line delineates the margin of the recovery. Images were captured at 5× magnification. *B*, Matrigel tube formation assay was performed to assess the effect of ghrelin on angiogenesis. *C* and *D*, graphical representation summarizing data from four different experiments in endothelial cells. Ghrelin significantly improves the migration and tube formation of endothelial cells under LPS insult condition. N = 6, * $p < 0.05$ compared with the control group, # $p < 0.05$ compared with the LPS group. LPS, lipopolysaccharide.

showed that VE-cadherin expression in the LPS group was reduced compared with that in the control group. However, compared with the LPS group, the expression of VE-cadherin

was increased in the ghrelin + LPS group (Fig. 7, E and F). In addition, LY294002 obviously decreased the expression of VE-cadherin increased by ghrelin. The results implied that

Ghrelin, acute respiratory distress syndrome

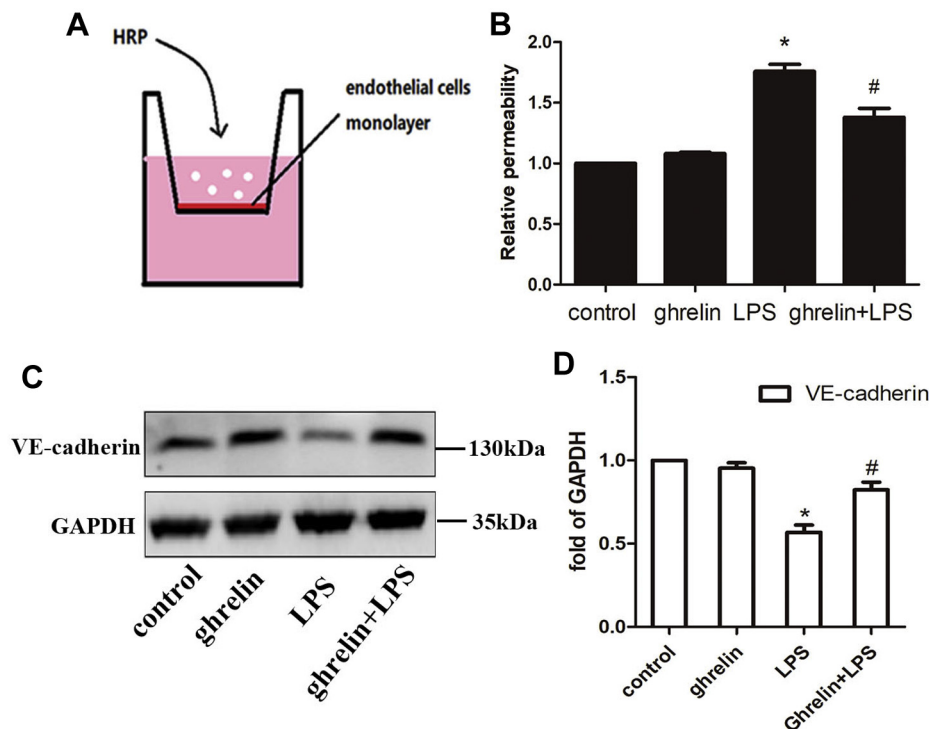


Figure 5. Ghrelin stabilized endothelial cell-cell adherens junctions after LPS insult in EA.hy 926 cells. *A* and *B*, transwell assay was performed to indicate pretreatment with ghrelin before insulting by LPS reduced the permeability of endothelial cell junction. *B*, the absorbance value of VE-cadherin in tissue. *C*, Western blot analysis showed that ghrelin enhanced the total protein expression of VE-cadherin under LPS insult conditions. *D*, the relative abundances of protein bands were quantified by measuring the corresponding band intensities; the relative values are expressed normalized to VE-cadherin signals as shown in the bar graphs. The VE-cadherin level was lower in the LPS-treated group than in the control group. As expected, the ghrelin + LPS group exhibited higher expression than in the LPS group. Values are expressed as the mean \pm SEM, $n = 6$ per group. * $p < 0.05$ compared with the control group, # $p < 0.05$ compared with the LPS group. LPS, lipopolysaccharide; VE-cadherin, vascular endothelial cadherin.

ghrelin might affect VE-cadherin expression through PI3K/Akt signaling pathway.

Discussion

In this study, we evaluated the roles of ghrelin in ARDS in a mouse model *in vivo* and in cells *in vitro*. Our results showed that ghrelin protected against LPS-induced ARDS by improving the pulmonary vascular endothelial barrier, providing insights into the potential applications of ghrelin as a therapeutic target in ARDS.

According to a study by Vila *et al.*, (15) ghrelin is one of the first hormones to show a rapid increase after LPS administration, indicating that ghrelin levels *in vivo* may be related to inflammatory diseases caused by LPS. Administration of exogenous ghrelin exerts beneficial effects on LPS-induced ARDS (16). In this study, we found that delivery of ghrelin attenuated lung injury in mouse models of ARDS, similar to previous studies. However, ghrelin is typically shown to exert protective effects on LPS-induced ARDS through blocking inflammation, including inhibiting the nuclear factor- κ B pathway and suppressing proinflammatory cytokine production in lung macrophages (17, 18).

Interestingly, we observed that ghrelin reversed the reduction of VE-cadherin protein caused by LPS. VE-cadherin is a member of the cadherin family that is expressed in different types of vascular endothelial cells. VE-cadherin plays key roles

in maintaining the integrity of endothelial cells barrier (19). In contrast to previous studies, we found that ghrelin protected the endothelial cell barrier by increasing the expression of VE-cadherin, thus exhibiting protective effects in LPS-induced ARDS.

Moreover, ghrelin had dual effects on endothelial cells at different concentrations; at concentrations of less than 100 nM, cell viability increased, whereas at concentrations of 1000 nM or more, cell viability decreased (Fig. 2B and Fig. S1), which is consistent with the study conducted by Jeffery (20).

ARDS is characterized by widespread injury to the alveolar-capillary barrier, resulting in increasing permeability (21). The importance of the pulmonary endothelial barrier in ARDS has been demonstrated (22). Therefore, a comprehensive understanding of the mechanisms that are involved in the protection of the endothelial barrier is essential for the development of therapeutic strategies to treat ARDS. Ghrelin, as a novel immunomodulatory factor that directly blocks the secretion of inflammatory mediators of sepsis, participates in regulating apoptosis, inflammation, cell proliferation, and angiogenesis in many *in vivo* and *in vitro* studies (16, 23–25). Because the integrity of the endothelial cell barrier depends on affinity interactions between adjacent endothelial cells through intercellular junctions (tight junctions and adhesive), the decreased cell number and disrupted interendothelial junctions induced by LPS could cause severe disruption of the endothelial cell

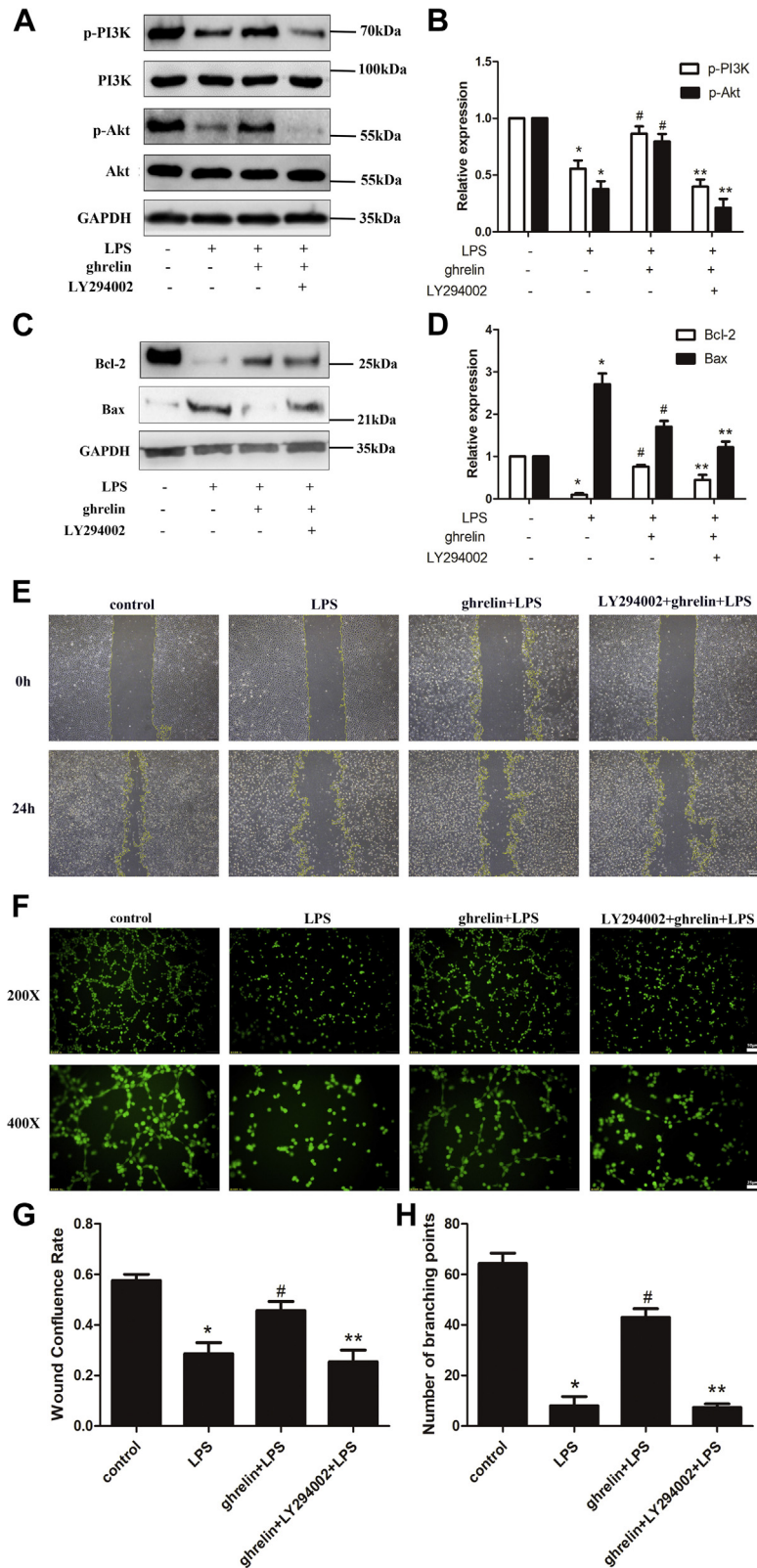


Figure 6. PI3K/AKT activation was involved in ghrelin-mediated lung endothelial cell barrier protection *in vitro*. The PI3K inhibitor, LY294002 (20 μ M), was added 30 min before ghrelin (100 nM) treatment. LPS was added 30 min after ghrelin treatment. *A* and *B*, Western blot analysis showed that ghrelin participated in the activation of the PI3K/AKT pathway, which was diminished under LPS insulting, and LY294002 reversed this effect. *C* and *D*, Western blot analysis showed that LY294002 inhibited the antiapoptotic protein Bcl-2 and proapoptotic protein Bax. *E*, the scratch-wound test indicated that the motility of endothelial cells was inhibited by adding LY294002. *F*, tube formation assay suggest that ghrelin promotes the vascular tube formation under LPS exposure but is reversed by the PI3K inhibitor LY294002. *G* and *H*, quantitative analysis of the wound confluence rates and numbers of tube formation are shown in the bar graphs. The data are presented as the mean \pm SEM, $n = 6$, * $p < 0.05$ compared with the control group, # $p < 0.05$ compared with the LPS group, ** $p < 0.05$ compared with the ghrelin + LPS group. LPS, lipopolysaccharide.

Ghrelin, acute respiratory distress syndrome

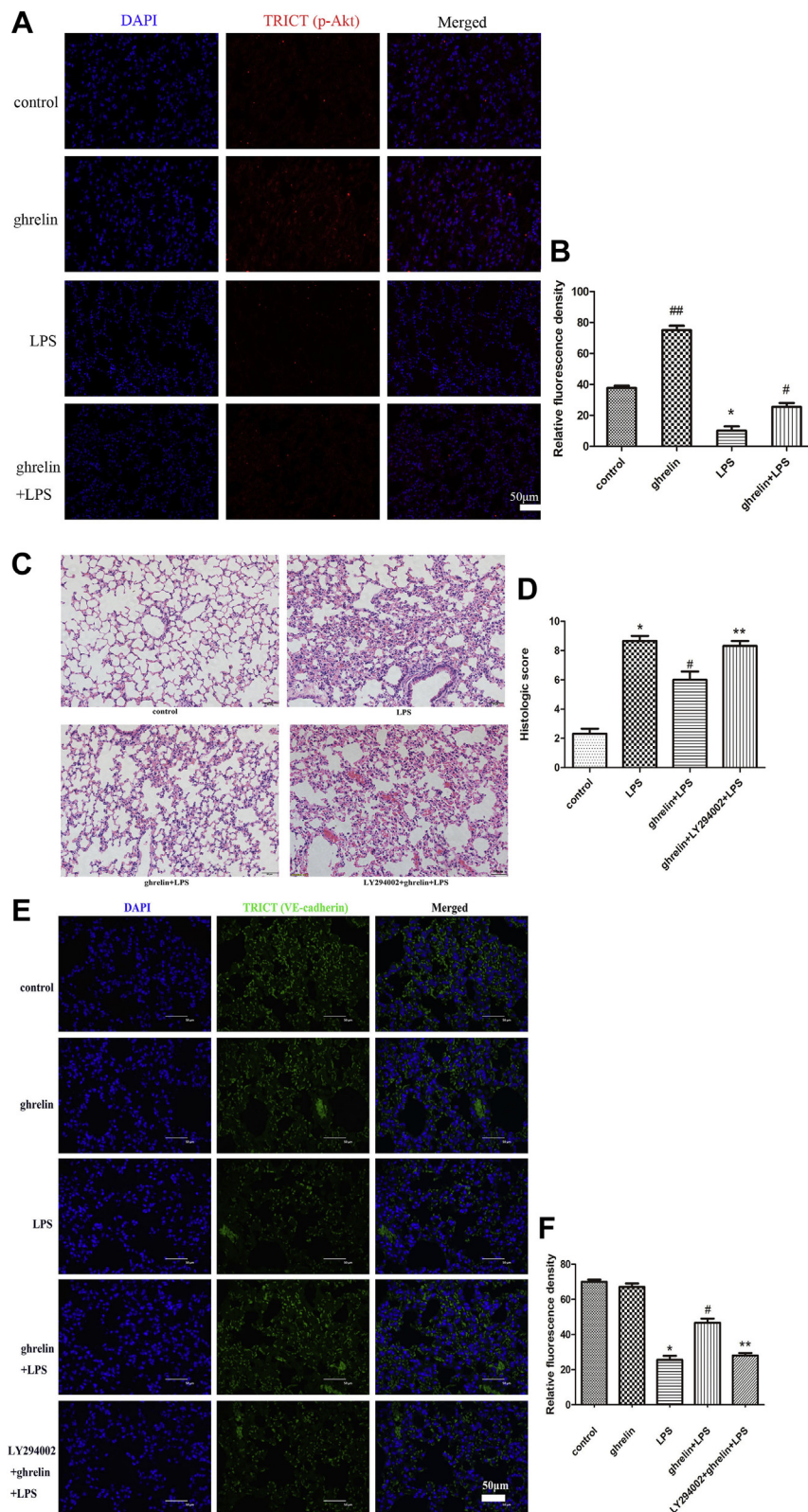


Figure 7. PI3K/AKT activation was involved in ghrelin-mediated protection of lung injury *in vivo*. A, immunofluorescence staining of p-AKT showed that increased pAkt in the ghrelin treated but not the LPS-only treated lungs. Red (TRICT) represents p-AKT, and blue represents nuclei. Mice divided into four groups were pretreated with or without ghrelin and subjected to intranasal injection with LPS (3 mg/kg) or dimethyl sulfoxide (DMSO), including the control group, LPS group, ghrelin group, and LPS + ghrelin group. B, the absorbance value of p-AKT in cells. Three slices of each mouse were used, and the observer randomly observed and photographed four fields of view. The observers were blinded to each experimental group. Data are expressed as the mean \pm SEM, $n = 4$, ^{##} $p < 0.05$ compared with the LPS group, ^{*} $p < 0.05$ compared with the control group, [#] $p < 0.05$ compared with the LPS group. C, H&E staining (magnification, $\times 200$) showed that LY294002 aggravated histological injury in LPS-induced ARDS mice ($n = 6$ independent mice from each group analyzed in triplicate). Mice divided into four groups were pretreated with or without ghrelin and subjected to intranasal injection with LPS (3 mg/kg) or

barrier (4, 26). Taken together, our findings demonstrated that these potential mechanisms may be related to endothelial cell barrier dysfunction during the development of ARDS. Therefore, we believe that antiapoptotic effects, promotion of cell migration, improvement of tube formation ability, and reduction of endothelial permeability may be beneficial for restoration of the endothelial cell barrier. Ghrelin exerts antiapoptotic effects by decreasing Bax and increasing Bcl-2 activities in various cells, including cardiomyocytes, neuronal cells, and human microvascular endothelial cells (27–29). In our study, we found that administration of ghrelin effectively inhibited the LPS-induced increase in apoptosis in ARDS through three experimental methods, including TUNEL assays, flow cytometry, and Western blotting, indicating the antiapoptotic effects of ghrelin *in vitro*. The effects of ghrelin on regulating cell migration and angiogenesis have mainly focused on cancer (30), and little is known regarding the roles of ghrelin in promoting cell migration and angiogenesis in ARDS. Our data suggested that ghrelin not only promoted cell migration but also increased tube formation in endothelial cells after LPS exposure. To eliminate the influence of cell proliferation, we use serum-free medium in the scratch experiment. In the lungs, increased endothelial permeability can lead to acute lung injury. Consistent with our *in vivo* results, we confirmed that the level of VE-cadherin protein was markedly decreased after exposure to LPS *in vitro* and that ghrelin administration could reverse this effect. Because the ghrelin group has been established in the previous phenomenon part to confirm the effect of adding ghrelin alone, the ghrelin group has not been set again in the latter part.

The PI3K/AKT pathway regulates cell growth, apoptosis, angiogenesis, and cell migration. Many studies have shown that the PI3K/AKT pathway plays key roles in lung injury (31). In addition, ghrelin inhibits hypoxia-induced injury and apoptosis of pulmonary artery endothelial cells through activating the PI3K/AKT signaling pathway (27). Here, consistent with previous findings, we showed that treatment of endothelial cells with ghrelin activated the PI3K/AKT signaling pathway, upregulated the antiapoptotic protein Bcl-2, and downregulated the proapoptotic protein Bax in LPS-induced lung injury. Furthermore, our results revealed that the PI3K inhibitor LY294002 partially reversed the protective effects of ghrelin on LPS-induced endothelial barrier disorder, including inhibition of endothelial cell migration and differentiation. Taken together, these results showed that ghrelin protected against LPS-induced ARDS and endothelial barrier dysfunction partially through the PI3K/AKT signaling pathway. To distinguish whether the PI3K-dependent effect of ghrelin in the lung is indeed mediated by endothelial cells, an

immunofluorescence experiment of VE-cadherin protein was conducted. Because the VE-cadherin is a transmembrane adhesion protein specifically expressed on the surface of vascular endothelial cells, the expression of VE-cadherin represented the endothelial cells. The immunofluorescence results showed that LY294002 obviously decreased the expression of VE-cadherin increased by ghrelin, which implied that there was a PI3K-dependent effect of ghrelin in the endothelial cells.

Nevertheless, there are still some limitations in our study to be addressed in future studies. First, our study only used VE-cadherin staining experiment to show the PI3K-dependent effect of ghrelin in the lung mediated by the endothelial cells. However, whether macrophage cells play a protective role of ghrelin in lung through PI3K pathway still remains unknown. In addition, the PI3K/AKT signaling pathway is probably not the unique potential mechanism. A recent study suggested that ghrelin protected human umbilical vein endothelial cells by activating the GHS-R1a and mammalian target of rapamycin/p70S6K signaling pathways (32). In addition, Liao *et al.* (33) suggested that ghrelin attenuated endothelial apoptosis induced by high glucose/high lipid concentrations *via* inhibition of the c-Jun N-terminal kinase 1/2 and p38 signaling pathways. Therefore, additional studies are needed to fully elucidate the mechanisms involved in these processes.

Conclusion

Collectively, our research indicated that ghrelin exhibited protective effects against LPS-induced ARDS on the pulmonary vascular endothelial barrier by inhibiting apoptosis and promoting cell migration and differentiation, which could have implications in the clinical treatment of patients with ARDS.

However, our study had some limitations. First, we exposed mice to LPS injection intranasally in an ARDS model. However, ARDS is a complicated state characterized by a combination of gram-negative and gram-positive infections. Hence, our model could not thoroughly explain the full mechanisms underlying ARDS-associated endothelial cell barrier dysfunction.

Experimental procedures

Preparation of reagents

Dulbecco's modified Eagle's medium (DMEM; Gibco, Thermo Fisher) supplemented with 10% fetal bovine serum (FBS) was used to culture cells. LPS (O127:B8) obtained from Sigma Chemical Co was dissolved in distilled water to a final concentration of 1 µg/ml. Ghrelin was purchased from Tocris

DMSO, including the control group, LPS group, ghrelin + LPS group, and ghrelin + LY294002 + LPS group. PI3K inhibitor, LY294002, dissolved in DMSO was injected into mice 1 h before LPS or PBS instillation through the tail vein. *D*, lung injury scores were utilized for quantitative analysis of lung histopathologic damage. *E*, immunofluorescence staining of VE-cadherin showed that ghrelin reversed the LPS-induced decrease in the expression of VE-cadherin, but this effect disappeared after adding LY294002. *Green* (TRITC) represents VE-cadherin, and *blue* represents nuclei. Mice divided into five groups were pretreated with or without ghrelin and subjected to intranasal injection with LPS (3 mg/kg) or DMSO, including the control group, ghrelin group, LPS group, ghrelin + LPS group, and ghrelin + LY294002 + LPS group. *F*, the absorbance value of VE-cadherin in cells. Three slices of each mouse were used, and the observer randomly observed and photographed six fields of view. The observers were blinded to each experimental group. Data are expressed as the mean ± SEM, *n* = 6, **p* < 0.05 compared with the control group, #*p* < 0.05 compared with the LPS group, ***p* < 0.05 compared with the ghrelin + LPS group. ARDS, acute respiratory distress syndrome; LPS, lipopolysaccharide; VE-cadherin, vascular endothelial cadherin.

Ghrelin, acute respiratory distress syndrome

(cat. no. 1463; Tocris) and was formulated into a solution with a concentration of 0.1 nmol/ml. CCK-8 assays (APExBIO) were used to determine cell viability. TUNEL assays (KeyGen Biotech Co, Ltd) and an Annexin V-FITC/PI apoptosis detection kit (BestBio) were also used. Growth factor-reduced Matrigel Basement Membrane Matrix was purchased from Corning Co. All antibodies, secondary Alexa Fluor 594-conjugated goat anti-rabbit IgG, and the PI3K inhibitor LY294002 were purchased from Cell Signaling Technology.

Mouse models of ARDS

The animals were purchased from the animal experiment center of Sun Yat-Sen University and were housed in a standard animal facility under a 12/12 h light/dark cycle with *ad libitum* access to food and water. The temperature was controlled at 23 to 24 °C. Experiments were performed with specific pathogen-free-grade 8-week-old BALB/c mice (Department of Laboratory Center, the First Affiliated Hospital of Sun Yat-sen University). Mice were randomly divided into four treatment groups, as follows: control group, received sterile saline *via* the tail vein and intranasal administration as a control; ghrelin group, received ghrelin *via* the tail vein and normal saline *via* intranasal administration; LPS group, received LPS *via* intranasal administration and normal saline *via* the tail vein; and ghrelin + LPS group, treated with ghrelin *via* the tail vein and LPS *via* intranasal administration. Mice were first slightly anesthetized with isoflurane, and LPS (3 mg/kg) was then instilled nasally to induce lung injury. Ghrelin (40 nmol/kg) was administered intravenously *via* the tail vein 30 min before the administration of LPS. The doses of ghrelin and LPS used in animal models were determined according to our previous studies (34). At 24 h after LPS injection, mice were sacrificed, and lung tissues were harvested and kept in 4% paraformaldehyde for subsequent experiments. All animal experiments were approved by the Institutional Animal Care and the Medical Ethical Committee of the First Affiliated Hospital of Sun Yat-sen University ([2019]254).

Histological analysis

To assess histological changes in lung tissues, lungs obtained from different groups were fixed with 4% paraformaldehyde, embedded in paraffin, and cut into 4- μ m-thick sections. After dewaxing and dehydration, sections were stained with H&E using histological examination and were then observed with an optical microscope (Olympus). VE-cadherin protein and p-Akt protein were also detected by *situ* immunohistochemical staining. After dewaxing and dehydration, they were blocked with the QuickBlock blocking solution (Beyotime, catalog number: P0252FT) for 10 min, and then, the primary antibody was added overnight. Finally, the fluorescent-labeled secondary antibody was added. The stain in each group was observed with a fluorescence microscope (Olympus), and the average fluorescence intensity was calculated using the ImageJ analysis system. To control the density of cells in each well, the cell suspension was mixed carefully before cell seeding and cultured under the same conditions.

Equal 4',6-diamidino-2-phenylindole signals fields were chosen to avoid the variation in the cell density/number per field. The calculation formula is mean gray value/integrated density (35). Histopathological scoring system of the lung issue was performed according to the following standard: absent, 0; mild (<25% field), 1; moderate (25%–50% field), 2; severe (>50% field), 3. Hemorrhage, edema, and leukocyte infiltration were used as criteria for lung injury (9, 36).

Cell culture and treatment

EA.hy 926 human umbilical vein endothelial cells were purchased from KeyGen Biotech Co and were cultured in DMEM supplemented with 10% FBS. Cells were divided into the control group, ghrelin group, LPS group, and ghrelin + LPS group. Cells in the control group receive no treatment or treated with dimethyl sulfoxide as a negative control, whereas cells in the LPS group were treated with LPS for 24 h as a positive control. Only ghrelin was added in the ghrelin group. Cells in the ghrelin + LPS group cells were stimulated with LPS (150 μ g/ml) for 24 h after pretreatment with ghrelin for 30 min. To verify the protective roles of ghrelin in endothelial cell barrier function *via* the PI3K/AKT pathway, we also evaluated cells treated with LY294002, ghrelin, and LPS. LY294002 was used at a concentration of 10 μ M dissolved in dimethyl sulfoxide based on our preliminary experiments.

CCK-8 assays

EA.hy 926 cells (1×10^4 cells/well) were seeded in 96-well plates and allowed to grow for 24 h. Cells were then treated with ghrelin (0.01~1000 nM), LPS (10~150 μ g/ml), and LY294002 (2~8 μ M) for 24 h. Cell viability was detected using CCK-8 assays. Subsequently, the absorbance was measured at 450 nm using a microplate reader.

Apoptosis assays

TUNEL assays and flow cytometry were conducted to evaluate apoptosis. A TUNEL Detection Kit (KeyGen Biotech Co, Ltd) was used according to the manufacturer's instructions. 4',6-Diamidino-2-phenylindole staining was used to identify nuclei, whereas TUNEL staining was used to identify dead cells. TUNEL-positive cells were counted in six different fields in each slide.

To further quantify apoptosis, Annexin V-FITC/PI staining was also performed. Cells were cultured in six-well plates at 1×10^6 cells/well and then pretreated with or without LY294002 and ghrelin for 30 min. Subsequently, cells were treated with 150 μ g/ml LPS. After 24 h, cells were collected, washed twice with PBS, and stained with Annexin V-FITC/PI in the binding buffer in the dark at room temperature (RT). Finally, a flow cytometry system was used to analyze the stained cells. The flow cytometry experiment gate was set according to the analysis of the untreated cells in the control group and the single-stained control after cell staining with Annexin V and PI, respectively.

Tube formation assays

Before adding EA.hy 926 cells, growth factor–reduced Matrigel (200 μ l) was polymerized in the wells of a 24-well plate at 37 °C for 30 min. EA.hy 926 cells (2×10^5) in 300 μ l DMEM supplemented with 10% FBS were dispensed into each well with or without ghrelin (100 nM) and LPS (150 μ g/ml). Calcein AM fluorescent dye was used to enhance the visibility of tube and network formation in Matrigel. The tubular structure was examined under microscopy 3 h after cell seeding. The degree of tube formation was quantified by counting the vascular cross points in three randomly selected fields of view in each well.

Wound scratch assays

EA.hy 926 cells were seeded in 6-well culture plates at a density of 1×10^6 cells/well and grown to confluence. The cell monolayers were scratched with a 200- μ l pipette tip. Cells were then washed once with PBS, and the medium was replaced with fresh serum-free medium or different treatments as described. Images of the scratched wounds were taken immediately after wounding. To observe cell migration, cell monolayers were imaged again at 24 h after wounding. ImageJ software was utilized to determine the percentage of wound closure. The wound healing percentage formula is (0-h scratch area – 24-h scratch area)/0-h scratch area \times 100%.

Endothelial cell permeability assay

Transwell permeability assays were used to measure the permeability of macromolecules for studying endothelial cell permeability (37). First, 2×10^5 EA.hy926 cells in 300 μ l medium were seeded in 6.5-mm transwell inserts and incubated for 5 days to ensure the cells formed a confluent monolayer. The medium was replaced with a fresh medium every 2 days. Five days later, the medium was aspirated from the top chambers and refilled with medium containing streptavidin-horseradish peroxidase. After 5 min of incubation, 20- μ l medium from the lower chamber was collected and moved to a new 96-well plate. Each condition was tested in triplicate. TMB substrate was added to each well, and cells were incubated for 5 min to stabilize the reaction at RT. After adding 25- μ l stop solution (Sigma-Aldrich, catalog number: 30743) to each well, the absorption was determined at 450 nm with a microplate reader.

Western blotting

Proteins were extracted from cells in the RIPA lysis buffer containing protease inhibitors (Beyotime, catalog number: ST506). Proteins were separated by SDS-PAGE (concentrated gel 80 V, 30 min, when the prestained marker starts to separate, 120 V, 1 h) and transferred to polyvinylidene difluoride membranes (300 mA, 90 min). The membranes were then blocked with the QuickBlock blocking buffer (Beyotime, catalog number: P0252FT) at RT for 10 min and incubated with the corresponding primary antibodies (*i.e.*, anti-AKT, anti-phospho-AKT, anti-PI3K, anti-phospho-PI3K anti-Bcl-2, anti-Bax, and anti-VE-cadherin antibodies diluted 1:1000;

anti-glyceraldehyde 3-phosphate dehydrogenase antibodies diluted 1:2000) overnight at 4 °C. The membranes were washed three times for 5 min each time with TBST and then incubated with secondary antibodies conjugated to horseradish peroxidase at RT for 1 h. Finally, the chemiluminescent signals were visualized using an ImageQuant LAS 4000 mini system (General Electric Company).

Statistical analysis

All quantitative data are presented as the means \pm SEM. All statistical analyses were performed using SPSS 20.0 statistical software. For comparisons of two groups, independent Student's *t*-tests were performed; for comparisons of multiple groups, one-way ANOVA and subsequent Student–Newman–Keuls tests were performed. Results with *p* values of less than 0.05 were considered statistically significant.

Data availability

All data generated or analyzed during this study are included in this published article (and its supplementary information files).

Supporting information—This article contains [supporting information](#).

Acknowledgments—This work was supported by the National Natural Science Foundation of China (Grant 81670066, 81772302), Guangdong Basic and Applied Basic Research Foundation (Grant 2019A1515011198), the Science and Technology Program of Guangzhou City (Grant 2014Y2-00136/201803010122), and the Guangdong Science and Technology Program (Grant 2019A030317003).

Author contributions—L. Z. and S. G. data curation; L. Z., S. G., W. H., C. X., and M. Z. methodology; L. Z. and S. G. writing—original draft; L. Z., S. G., and W. H. formal analysis; L. Z., S. G., W. H., and Q. C. investigation; W. H. and Q. C. software; W. H., Q. C., C. X., and M. Z. supervision; Q. C. validation; C. X. and M. Z. conceptualization; C. X. writing—review and editing; M. Z. resources; M. Z. funding acquisition; M. Z. project administration.

Conflict of interest—The authors declare that they have no conflicts of interest with the contents of this article.

Abbreviations—The abbreviations used are: ARDS, acute respiratory distress syndrome; CCK-8, Cell Counting Kit-8; FBS, fetal bovine serum; LPS, lipopolysaccharide; PI, propidium iodide; VE-cadherin, vascular endothelial cadherin.

References

1. Yuan, S. Y., and Rigor, R. R. (2011). In *Regulation of endothelial barrier function*, Morgan and Claypool Life Sciences, San Rafael, CA: 146
2. Narula, T., and Deboisblanc, B. P. (2015) Ghrelin in critical illness. *Am. J. Respir. Cell Mol. Biol.* 53, 437–442
3. Matthay, M. A., Zemans, R. L., Zimmerman, G. A., Arabi, Y. M., Beitler, J. R., Mercat, A., Herridge, M., Randolph, A. G., and Calfee, C. S. (2019) Acute respiratory distress syndrome. *Nat. Rev. Dis. Primers* 5, 18

Ghrelin, acute respiratory distress syndrome

- Liu, H., Yu, X., Yu, S., and Kou, J. (2015) Molecular mechanisms in lipopolysaccharide-induced pulmonary endothelial barrier dysfunction. *Int. Immunopharmacol.* **29**, 937–946
- Zheng, X., Zhang, W., and Hu, X. (2018) Different concentrations of lipopolysaccharide regulate barrier function through the PI3K/AKT signalling pathway in human pulmonary microvascular endothelial cells. *Sci. Rep.* **8**, 9963
- Qi, D., Tang, X., He, J., Wang, D., Zhao, Y., Deng, W., Deng, X., Zhou, G., Xia, J., Zhong, X., and Pu, S. (2016) Omentin protects against LPS-induced ARDS through suppressing pulmonary inflammation and promoting endothelial barrier via an AKT/eNOS-dependent mechanism. *Cell Death Dis.* **7**, e2360
- Laakkonen, J. P., Lappalainen, J. P., Theelen, T. L., Toivanen, P. I., Nieminen, T., Jauhiainen, S., Kaikkonen, M. U., Sluimer, J. C., and Ylä-Herttua, S. (2017) Differential regulation of angiogenic cellular processes and claudin-5 by histamine and VEGF via PI3K-signaling, transcription factor SNAI2 and interleukin-8. *Angiogenesis* **20**, 109–124
- Wu, R., Dong, W., Cui, X., Zhou, M., Simms, H. H., Ravikumar, T. S., and Wang, P. (2007) Ghrelin down-regulates proinflammatory cytokines in sepsis through activation of the vagus nerve. *Ann. Surg.* **245**, 480–486
- Zhou, X., and Xue, C. (2010) Ghrelin attenuates acute pancreatitis-induced lung injury and inhibits substance P expression. *Am. J. Med. Sci.* **339**, 49–54
- Imazu, Y., Yanagi, S., Miyoshi, K., Tsubouchi, H., Yamashita, S., Matsu-moto, N., Ashitani, J., Kangawa, K., and Nakazato, M. (2011) Ghrelin ameliorates bleomycin-induced acute lung injury by protecting alveolar epithelial cells and suppressing lung inflammation. *Eur. J. Pharmacol.* **672**, 153–158
- Li, B., Zeng, M., He, W., Huang, X., Luo, L., Zhang, H., and Deng, D. Y. (2015) Ghrelin protects alveolar macrophages against lipopolysaccharide-induced apoptosis through growth hormone secretagogue receptor 1a-dependent c-Jun N-terminal kinase and Wnt/ β -catenin signaling and suppresses lung inflammation. *Endocrinology* **156**, 203–217
- Lin, T. C., Liu, Y. P., Chan, Y. C., Su, C. Y., Lin, Y. F., Hsu, S. L., Yang, C. S., and Hsiao, M. (2015) Ghrelin promotes renal cell carcinoma metastasis via Snail activation and is associated with poor prognosis. *J. Pathol.* **237**, 50–61
- Waseem, T., Duxbury, M., Ashley, S. W., and Robinson, M. K. (2014) Ghrelin promotes intestinal epithelial cell proliferation through PI3K/AKT pathway and EGFR trans-activation both converging to ERK 1/2 phosphorylation. *Peptides* **52**, 113–121
- Zhu, J., Yao, J., Huang, R., Wang, Y., Jia, M., and Huang, Y. (2018) Ghrelin promotes human non-small cell lung cancer A549 cell proliferation through PI3K/AKT/mTOR/P70S6K and ERK signaling pathways. *Biochem. Biophys. Res. Commun.* **498**, 616–620
- Vila, G., Maier, C., Riedl, M., Nowotny, P., Ludvik, B., Luger, A., and Clodi, M. (2007) Bacterial endotoxin induces biphasic changes in plasma ghrelin in healthy humans. *J. Clin. Endocrinol. Metab.* **92**, 3930–3934
- Chorny, A., Anderson, P., Gonzalez-Rey, E., and Delgado, M. (2008) Ghrelin protects against experimental sepsis by inhibiting high-mobility group box 1 release and by killing bacteria. *J. Immunol.* **180**, 8369–8377
- Wu, R., Dong, W., Zhou, M., Zhang, F., Marini, C. P., Ravikumar, T. S., and Wang, P. (2007) Ghrelin attenuates sepsis-induced acute lung injury and mortality in rats. *Am. J. Respir. Crit. Care Med.* **176**, 805–813
- Chen, J., Liu, X., Shu, Q., Li, S., and Luo, F. (2008) Ghrelin attenuates lipopolysaccharide-induced acute lung injury through NO pathway. *Med. Sci. Monit.* **14**, BR141–BR146
- Giannotta, M., Trani, M., and Dejana, E. (2013) VE-cadherin and endothelial adherens junctions: Active guardians of vascular integrity. *Dev. Cell* **26**, 441–454
- Jeffery, P. L., Murray, R. E., Yeh, A. H., McNamara, J. F., Duncan, R. P., Francis, G. D., Herington, A. C., and Chopin, L. K. (2005) Expression and function of the ghrelin axis, including a novel preproghrelin isoform, in human breast cancer tissues and cell lines. *Endocr. Relat. Cancer* **12**, 839–850
- Matthay, M. A., and Zemans, R. L. (2011) The acute respiratory distress syndrome: Pathogenesis and treatment. *Annu. Rev. Pathol.* **6**, 147–163
- Muller-Redetzky, H. C., Suttrop, N., and Witzenrath, M. (2014) Dynamics of pulmonary endothelial barrier function in acute inflammation: Mechanisms and therapeutic perspectives. *Cell Tissue Res.* **355**, 657–673
- Koyuturk, M., Sacan, O., Karabulut, S., Turk, N., Bolkent, S., Yanardag, R., and Bolkent, S. (2015) The role of ghrelin on apoptosis, cell proliferation and oxidant-antioxidant system in the liver of neonatal diabetic rats. *Cell Biol. Int.* **39**, 834–841
- Katare, R., Rawal, S., Munasinghe, P. E., Tsuchimochi, H., Inagaki, T., Fujii, Y., Dixit, P., Umetani, K., Kangawa, K., Shirai, M., and Schwenke, D. O. (2016) Ghrelin promotes functional angiogenesis in a mouse model of critical limb ischemia through activation of proangiogenic microRNAs. *Endocrinology* **157**, 432–445
- Li, B., Zeng, M., Zheng, H., Huang, C., He, W., Lu, G., Li, X., Chen, Y., and Xie, R. (2016) Effects of ghrelin on the apoptosis of human neutrophils in vitro. *Int. J. Mol. Med.* **38**, 794–802
- Millar, F. R., Summers, C., Griffiths, M. J., Toshner, M. R., and Proudfoot, A. G. (2016) The pulmonary endothelium in acute respiratory distress syndrome: Insights and therapeutic opportunities. *Thorax* **71**, 462–473
- Yang, D., Liu, Z., Zhang, H., and Luo, Q. (2013) Ghrelin protects human pulmonary artery endothelial cells against hypoxia-induced injury via PI3-kinase/AKT. *Peptides* **42**, 112–117
- Kui, L., Weiwei, Z., Ling, L., Daikun, H., Guoming, Z., Linuo, Z., and Renming, H. (2009) Ghrelin inhibits apoptosis induced by high glucose and sodium palmitate in adult rat cardiomyocytes through the PI3K-AKT signaling pathway. *Regul. Pept.* **155**, 62–69
- Zhang, R., Yang, G., Wang, Q., Guo, F., and Wang, H. (2013) Acylated ghrelin protects hippocampal neurons in pilocarpine-induced seizures of immature rats by inhibiting cell apoptosis. *Mol. Biol. Rep.* **40**, 51–58
- Chopin, L. K., Seim, I., Walpole, C. M., and Herington, A. C. (2012) The ghrelin axis—does it have an appetite for cancer progression? *Endocr. Rev.* **33**, 849–891
- Medina-Tato, D. A., Ward, S. G., and Watson, M. L. (2007) Phosphoinositide 3-kinase signalling in lung disease: Leucocytes and beyond. *Immunology* **121**, 448–461
- Zhu, J., Zheng, C., Chen, J., Luo, J., Su, B., Huang, Y., Su, W., Li, Z., and Cui, T. (2014) Ghrelin protects human umbilical vein endothelial cells against high glucose-induced apoptosis via mTOR/P70S6K signaling pathway. *Peptides* **52**, 23–28
- Liao, P., Yang, D., Liu, D., and Zheng, Y. (2017) GLP-1 and ghrelin attenuate high glucose/high lipid-induced apoptosis and senescence of human microvascular endothelial cells. *Cell. Physiol. Biochem.* **44**, 1842–1855
- Zeng, M., He, W., Li, L., Li, B., Luo, L., Huang, X., Guan, K., and Chen, W. (2015) Ghrelin attenuates sepsis-associated acute lung injury oxidative stress in rats. *Inflammation* **38**, 683–690
- Jensen, E. C. (2013) Quantitative analysis of histological staining and fluorescence using ImageJ. *Anat. Rec. (Hoboken)* **296**, 378–381
- Li, Y., Wei, H., Yu, X., Li, J., and Han, Y. (2009) Establishment and evaluation of ARDS model in rats with refractory hypoxemia caused by endotoxin “twice hit”. *Chin. J. Pathophysiol.* **25**, 2235–2239
- Chen, H., and Yeh, T. (2017) *In vitro* assays for measuring endothelial permeability by transwells and electrical impedance systems. *Bio-protocol* **9**, e2273